



Unsteady oscillatory MHD boundary layer flow past a moving plate with mass transfer and binary chemical reaction

A. M. Okedoye¹ · S. O. Salawu²Received: 29 July 2019 / Accepted: 3 October 2019 / Published online: 9 November 2019
© Springer Nature Switzerland AG 2019

Abstract

In this work, we have studied analytically the heat and mass transfer of unsteady MHD natural convective flow past a motioning plate with binary chemical reaction. The flow surface spontaneously moves with unvaried velocity in the flow direction or opposite under the influence of magnetic field. We studied both frequency-dependent effects and “long-time” effects that would require non-practically long channels to be observed in steady flow. We also explored mathematically the important aspects of reactive fluid flow, especially the residence time flow behaviour, scale-up and scale-down procedures. From the present study, it is seen amongst others that temperature is enhanced as the fluid angular velocity rises which leads to maximum temperature in the body of the liquid. It is discovered that mean velocity decrease with a rise in the species reaction and reaction order. The graphical results representing the governing flow parameters effect were presented and discussed. The flow conditions at the wall were also investigated, presented and described.

Keywords Magnetohydrodynamic flows (MHD) · Boundary layer · Oscillating plate · Binary chemical reaction

1 Introduction

Several reacting processes contain chemical species with different chemical kinetics; such occur in toxic pollution control and geothermal. The relations between chemical reactions and species transfer are mostly very compound, and this can be noticed in the generation and utilization of species reactant at various degrees both in the contest of the flow liquid and concentration transfer, Salawu et al. [1]. The investigation into the flow of hydromagnetic fluid and energy transfer has gotten significant consideration recently because of its wide usage in technology and engineering processes which include nuclear reactors, studies of plasma, extractions of geothermal energy, MHD generator and so on, Hassan et al. [2]. MHD is the multi-disciplinary study of the fluid flow of an electrically conducting fluid in electromagnetic fields, such fluids include plasmas,

liquid metals, and urine (salt water). MHD over a moving plate has several applications in in stellar and solar structures, astrophysics and geophysics, radio propagation, interstellar matter, ionosphere and so on. Flow of convective fluid has a well pronounced modern application in geothermal systems, granular and fibre and many more. Buoyancy effect is very significant in the domain where variances between air and land heat gives rise to complex flow patterns Salawu and Fatunmbi [3]. In nature, numerous transport processes occur where species and temperature transfer exists concurrently due to the combined effect of buoyancy forces as a result of chemical and thermal diffusions. Convective flows of transient oscillatory fluid assume a critical role in aerospace technology, turbo machinery and chemical engineering; such flows emerge because of unsteady boundary motion or unsteady temperature boundary. Additionally, temperature and free

✉ S. O. Salawu, kunlesalawu2@gmail.com; A. M. Okedoye, okedoye.akindele@fupre.edu.ng | ¹Department of Mathematics and Computer Science, Federal University of Petroleum Resources, Effurun, Nigeria. ²Department of Mathematics, Landmark University, Omu-Aran, Nigeria.



stream momentum can cause the flow unsteadiness. Unsteady rotating fluid flows have many possible applications and uses in nuclear mechanical engineering, dynamics of geophysical liquid and chemical processes.

Many researchers reported their findings in the area of thermal hydromagnetic fluid with buoyancy induced flows, and flows in rotating fluids as well as flow of chemical binary reactive fluid in the presence of activation energy. Some of the earliest studies in the aforementioned areas could be found in the work of Soundalgekar et al. [4], who examined the transient viscous, incompressible, rotating flow liquid over an infinite permeable wall. Bergstrom [5] reported on the oscillating flow of rotating fluid problem in a boundary layer past a vast half-plate. Other earlier works include [6–11]. Waqas et al. [12] reported on thermally developed Falkner–Skan bioconvection flow of a magnetized nanofluid in the presence of motile gyrotactic microorganism: Buongiorno's nanofluid model. The authors gave various aspects of involved physical quantities of the flow. Nguyen et al. [13] considered Macroscopic modeling for convection of Hybrid nanofluid with magnetic effects. From the results, it is found that radiation parameter and magnetic boosts the Nusselt number. Nguyen-Thoi et al. [14] investigated Analysis on the heat storage unit through a Y-shaped fin for solidification of NEPCM.

Not quit long, in the work of Maleque [15], the solution to an unsteady temperature and species transport of natural convective flow through permeable surface in a boundary layer was obtained using similarity solution. Maleque [16] investigated the impacts of the temperature dependent chemical reactive fluid and Arrhenius energy kinetic on the flow momentum, concentration and temperature. Awad et al. [17] solved transient rotating viscous, incompressible nonlinear coupled equations governing the flow over a stretching plate in the existence of Arrhenius kinetic and chemically binary reaction using the method of spectral relaxation. Mallikarjuna et al. [18] analyzed convective variable porosity of MHD rotating flow of mass and energy transfer in a vertical cone with chemical reaction. While Zhang et al. [19] examined radiative MHD nanofluid in a permeable medium with chemical reaction and surface variable heat flux. Abbas et al. [20] presented mass transfer in a thermal radiation of unsteady Casson stagnation fluid past an extending or contracting boundary layer surface. In the study, the Arrhenius kinetic and chemical binary reaction effect on a temperature dependent viscous fluid is considered. The work of Shafiqen et al. [21] reported on the effects of unidirectional Maxwell revolving flow of species and energy transfer over a stretching sheet. The authors presented proportionally mixed

binary concentration to both parameters fitted rate n , the reaction rate r , activation energy E , and rotation k . It was noticed that the parameters causes concentration solute distribution reduction.

Other most recent work include the work of Khan et al. [22] on energy and species transport on the flow of chemical reactive axisymmetric convection MHD Maxwell fluid flow propelled by isothermal widening disks and exothermal. Mabood et al. [23] reported on mass and temperature transfer of hydromagnetic stagnation nanofluids flow in porous media with chemical reaction, viscous dissipation and radiation while Rawat et al. [24] presented MHD micropolar fluid flow of energy and chemical species transport past a nonlinear elongating plate in a non-Darcy permeable medium with variable micro inertia density, heat flux and chemical reaction. Despite the effort of the earlier scholars, there is evolving requests for determination of the binary chemical reaction of unsteady natural convection MHD boundary layer flow past a moving sheet with mass and heat transfer due to its numerous applications in technology, engineering and industry.

2 Problem formulation

Examine an unsteady, viscous, incompressible, flow of conducting free convection fluid over a vertical non conducting infinite flat sheet in porous media. The flow is along x -axis in the upward vertically direction with y -axis is assumed perpendicular to the flow direction. A uniform strength magnetic field B_0 is introduced in the flow direction with the neglecting of the temperature field. Initially, the conducting fluid and sheet have equal temperature T_w in a fixed condition and fluid species level C_w at very points. The sheet begins oscillating with velocity U_0 at time $t > 0$ in its own plane. The flow concentration and temperature at C_w and T_w respectively raised in level as the plate oscillating. For an incompressible flow, the governing compactible continuity equation and MHD momentum flow equation in a porous medium is defined as

$$\operatorname{div} V = 0 \quad (1)$$

$$\rho \left(\frac{dV}{dt} \right) = \operatorname{div} T + J \times B - \frac{\mu \phi}{k} V \quad (2)$$

where B stands for magnetic field, $V = (u, v, w)$ represents the velocity vector, T is the stress Cauchy tensor, ρ denotes fluid density, J is the current density, d/dt is the material derivative, $k > 0$ connote permeable medium, and $\phi (0 < \phi < 1)$ is the porosity.

Under the Boussinesq's approximation, the continuity equation, the fluid momentum, energy and species equations are described as follows:

$$\frac{\partial v'}{\partial y} = 0 \tag{3}$$

$$\begin{aligned} \frac{\partial u'}{\partial t} + v \frac{\partial u'}{\partial y} = & -\frac{1}{\rho} \frac{\partial p}{\partial x} + \nu \frac{\partial^2 u'}{\partial y^2} + \frac{g\beta_T}{\rho} (T' - T_\infty) \\ & + \frac{g\beta_C}{\rho} (C' - C_\infty) + \frac{\delta B_0^2}{\rho} (U_\infty - u') \\ & - \frac{\nu}{k} (U_\infty - u') \end{aligned} \tag{4}$$

$$\rho C_p \left(\frac{\partial T'}{\partial t} + v \frac{\partial T'}{\partial y} \right) = k \frac{\partial^2 T'}{\partial y^2} + Q(T' - T_\infty) \tag{5}$$

$$\begin{aligned} \frac{\partial C'}{\partial t} + v \frac{\partial C'}{\partial y} = & D_m \frac{\partial^2 C'}{\partial y^2} - k_r (T' - T_\infty)^n \\ & \exp\left(-\frac{E_a}{k(T' - T_\infty)}\right) (C' - C_\infty) \end{aligned} \tag{6}$$

The boundary and initial conditions are equally stated as:

$$\begin{aligned} u' = U_0, \quad v' = v_w(t), \quad T' = T_w, \quad C' = C_w \quad \text{for } y, \quad t \leq 0 \\ u' = U_1, \quad T' = T_\infty + A_1 e^{i\omega t}, \quad C' = C_\infty + A_2 e^{i\omega t}, \quad y = 0, \quad t > 0 \\ u' \rightarrow U(t), \quad T' = T_\infty, \quad C' = C_\infty \quad \text{as } y \rightarrow \infty, \quad t > 0 \end{aligned} \tag{7}$$

Introducing the following dimensionless quantities

$$\begin{aligned} y' = \frac{y v_0}{\nu}, \quad u' = \frac{u}{U_0}, \quad t' = \frac{t v_0^2}{4\nu}, \quad U' = \frac{U}{U_0} \\ \omega' = \frac{4\omega\nu}{v_0^2}, \quad V = \frac{U_1}{U_0}, \quad \theta = \frac{T' - T_\infty}{T_w - T_\infty} \end{aligned} \tag{8}$$

All the physical quantities maintain their normal denotations.

Following Messiha [25], Eq. (3) on integration becomes

$$\begin{aligned} v'(t, y) = \text{constant} \\ \text{But at } t = 0, v'(t, y) = v_w(t) = -v_0(1 + \epsilon A e^{i\omega t}), \\ \Rightarrow v'(t, y) = -v_0(1 + \epsilon A e^{i\omega t}) \end{aligned} \tag{9}$$

The stream velocity is given by

$$U(t) = 1 + \epsilon e^{i\omega t}$$

At free stream, $u \rightarrow U, T \rightarrow T_\infty, C \rightarrow C_\infty$, thus from Eq. (4)

$$-\frac{1}{\rho} \frac{\partial p}{\partial x} = \frac{\partial U}{\partial t} = \frac{\partial}{\partial t} (\epsilon \omega e^{i\omega t})$$

Now using Eqs. (8) and (9), Eqs. (4)–(6) after dropping primes becomes

$$\begin{aligned} \frac{1}{4} \frac{\partial u}{\partial t} - (1 + \epsilon A e^{i\omega t}) \frac{\partial u}{\partial y} = & \epsilon \frac{i\omega}{4} e^{i\omega t} + \frac{\partial^2 u}{\partial y^2} \\ & + Gr\theta + Grc\theta - (M + k_p)(1 - u) \end{aligned} \tag{10}$$

$$\frac{1}{4} \frac{\partial \theta}{\partial t} - (1 + \epsilon A e^{i\omega t}) \frac{\partial \theta}{\partial y} = \frac{1}{Pr} \frac{\partial^2 \theta}{\partial y^2} + \delta\theta \tag{11}$$

$$\frac{1}{4} \frac{\partial \phi}{\partial t} - (1 + \epsilon A e^{i\omega t}) \frac{\partial \phi}{\partial y} = \frac{1}{Sc} \frac{\partial^2 \phi}{\partial y^2} - \epsilon \lambda \phi \theta^r e^{\frac{\theta}{1+\epsilon\theta}} \tag{12}$$

And the corresponding initial-boundary condition becomes

$$\begin{aligned} y = 0 : u = V, \quad \theta = 1 + \epsilon e^{i\omega t}, \quad \phi = 1 + \epsilon e^{i\omega t} \\ y \rightarrow \infty : u \rightarrow U, \quad \phi \rightarrow 0, \quad \theta \rightarrow 0 \end{aligned} \tag{13}$$

3 Method of solution

To solve Eqs. (10)–(12) with the initial boundary conditions of Eq. (13), we use perturbation in the neighborhood of the limiting surface, the one used by Lighthill [26]. The Velocity, specie concentration and temperature fields are given by the expressions

$$\begin{aligned} u(y, t) = f_0(y) + \epsilon A e^{i\omega t} f_1(y) \\ \theta(y, t) = h_0(y) + \epsilon A e^{i\omega t} h_1(y) \\ \phi(y, t) = g_0(y) + \epsilon A e^{i\omega t} g_1(y) \end{aligned} \tag{14}$$

Substituting Eq. (14) into Eqs. (10)–(13), separating the non-harmonic and harmonic terms and ignoring the coefficient of ϵ^2 , to get the mean velocity, mean temperature and chemical specie respectively;

$$f_0'' + f_0' + (M + k_p)f_0 = (M + k_p) - Grt_0 - Grch_0 \tag{15a}$$

$$g_0'' + Pr g_0' + Pr \delta g_0 = 0 \tag{15b}$$

$$h_0'' + Sch_0' - Sc \lambda g_0 h_0' e^{h_0} = 0 \tag{15c}$$

With boundary conditions

$$\begin{aligned} f_0 &= V, & g_0 &= 1, & h_0 &= 1, & y &= 0 \\ f_0 &\rightarrow 0, & g_0 &\rightarrow 0, & h_0 &\rightarrow 0, & y &\rightarrow \infty \end{aligned} \tag{15d}$$

And the oscillation part of the velocity, temperature and chemical specie are

$$f_1'' + f_1' + \left(M + k_p + \frac{i\omega}{4}\right)f_1 = -\frac{i\omega}{4} - Af_0' - Grtg_1 - Grch_1 \tag{16a}$$

$$g_1'' + Pr g_1' + Pr \left(\delta - \frac{i\omega}{4}\right)g_1 = -Pr Ag_0' \tag{16b}$$

$$h_1'' + Sch_1' - Sc \left(\frac{i\omega}{4} \lambda g_0' e^{g_0}\right)h_1 = -ScAh_0' + \lambda Sc(1 + rg_0^{-1})h_0 g_1 g_0' e^{g_0} \tag{16c}$$

Also the corresponding boundary conditions are given by the expressions:

$$\begin{aligned} f_1 &= g_1 = h_1 = 0, & y &= 0 \\ f_1 &\rightarrow 0, g_1 \rightarrow 0, & h_1 &\rightarrow 0, & y &\rightarrow \infty \end{aligned} \tag{16d}$$

The solutions of Eqs. 15a–c and 16a–c under the boundary conditions 15d and 16d respectively are

$$g_0(y) = e^{-my} \tag{17a}$$

$$h_0(y) = e^{-Scy} (1 - \lambda a_0 (1 - e^{-my})) \tag{17b}$$

$$f_0(y) = 1 + a_{13}e^{-cy} + a_{15}e^{-my} + a_{16}e^{-Scy} + a_{17}e^{-(m+Sc)y} \tag{17c}$$

$$g_1(y) = \frac{i\omega}{4} (e^{-m_1y} - e^{-my}) \tag{18a}$$

$$\begin{aligned} h_1(y) &= ia_1 e^{-Scy} + (a_3 + i(a_1 + a_4) + \lambda a_5) e^{-ny} + (a_3 + ia_4) e^{-(m+Sc)y} \\ &+ \lambda(a_6 e^{-n_2y} + a_7 e^{-n_3y} + a_8 e^{-n_4y} + a_9 e^{-(n_3+m_1)y} \\ &+ a_{10} e^{-(n_6+m_1)y} + a_{11} e^{-(n_2+m_1)y} + a_{12} e^{-n_5y}) \end{aligned} \tag{18b}$$

$$\begin{aligned} f_1(y) &= 1 + a_{19}e^{-c_1y} + a_{20}e^{-cy} + a_{21}e^{-my} + a_{22}e^{-Scy} + a_{23}e^{-m_1y} \\ &+ a_{24}e^{-(m+Sc)y} + a_{25}e^{-n_1y} + a_{26}e^{-n_2y} + a_{27}e^{-n_3y} + a_{28}e^{-n_4y} \\ &+ a_{29}e^{-(n_4+m_1)y} + a_{30}e^{-(n_6+m_1)y} + a_{31}e^{-(n_2+m_1)y} + a_{32}e^{-n_5y} \end{aligned} \tag{18c}$$

where $\delta \gg \frac{Pr-1}{Pr} \Rightarrow M \ll 1$, where $n_2 = Sc + m(r + 2)$, $n_3 = m(r + 1) + n_1$,

$$n_4 = Sc + m(r + 1), \quad n_5 = Sc + m(r + 3), \quad n_6 = rm + Sc$$

The functions $f_0(y), g_0(y)$ and $h_0(y)$ represented by Eqs. (17a)–(17c) are the mean momentum, energy and species fields respectively, and $f_1(y), g_1(y)$ and $h_1(y)$ represented by Eqs. (18a)–(18c) are the oscillatory flow rate, heat and concentration respectively.

We now substitute (17) and (18) into (4) to get expression for the flow rate, concentration and heat distribution as

$$\begin{aligned} u(y, t) &= 1 + a_{13}e^{-cy} + a_{15}e^{-my} + a_{16}e^{-Scy} \\ &+ a_{17}e^{-(m+Sc)y} + \epsilon(a_{19}e^{-(c_1+l_2)y} \\ &+ (b_{15} + lb_{16})e^{-cy} + (b_{17} + lb_{18})e^{-my} \\ &+ (b_{19} + lb_{20})e^{-Scy} + (b_{21} + lb_{22})e^{-(d_1+l_2)y} \\ &+ (b_{29} + lb_{30})e^{-n_3y} + (b_{23} + lb_{24})e^{-(m+Sc)y} \\ &+ (b_{25} + lb_{26})e^{-n_1y} + (b_{27} + lb_{28})e^{-n_2y} \\ &+ (b_{31} + lb_{32})e^{-n_4y} + (b_{33} + lb_{34})e^{-(n_4+d_1+l_2)y} \\ &+ (b_{35} + lb_{36})e^{-(n_6+d_1+l_2)y} + (b_{37} + lb_{38})e^{-(n_2+d_1+l_2)y} \\ &+ (b_{39} + lb_{40})e^{-n_5y} + (b_{41} + lb_{42})e^{i\omega t} \end{aligned} \tag{19}$$

$$\begin{aligned} \theta(y, t) &= e^{-Scy} (1 - \lambda a_0 (1 - e^{-my})) \\ &+ \epsilon((a_3 + l(a_1 + a_4) + \lambda a_5) e^{-(c_1+l_2)y} \\ &+ (a_3 + lb_4) e^{-(m+Sc)y} + la_1 e^{-Scy} \\ &+ \lambda((b_1 + lb_2) e^{-n_2y} + (b_3 + lb_4) e^{-n_3y} \\ &+ (b_5 + lb_6) e^{-n_4y} + (b_7 + lb_8) e^{-(n_4+d_1+l_2)y} \\ &+ (b_9 + lb_{10}) e^{-(n_6+d_1+l_2)y} \\ &+ (b_{11} + lb_{12}) e^{-(n_2+d_1+l_2)y} \\ &+ (b_{13} + lb_{14}) e^{-n_5y}) e^{i\omega t} \end{aligned} \tag{20}$$

$$\theta(y, t) = e^{-my} + \frac{1}{4} \epsilon \omega (e^{-m_1y} + e^{-my}) e^{i\omega t} \tag{21}$$

Maple software is applied to the above equations to split them into pairs of real and imaginary parts. From Eq. (19), the real part of the velocity can be expressed in terms of the unstable parts as

$$\begin{aligned} R(u(y, t)) &= 1 + a_{13}e^{-cy} + a_{15}e^{-my} + a_{16}e^{-Scy} + a_{17}e^{-(m+Sc)y} \\ &+ \epsilon(u_1 \cos \omega t - u_2 \sin \omega t) \end{aligned} \tag{22}$$

or

$$\begin{aligned} R(u(y, t)) &= 1 + a_{13}e^{-cy} + a_{15}e^{-my} + a_{16}e^{-Scy} \\ &+ a_{17}e^{-(m+Sc)y} + \epsilon u_{12} \cos(\omega t + \alpha_3) \end{aligned} \tag{23}$$

where

$$\begin{aligned}
 u_1 = & a_{19}e^{-c_1y} \cos y c_2 + b_{15}e^{-cy} + b_{17}e^{-my} + b_{19}e^{-Scy} + b_{21}e^{-d_1y} \cos d_2y + b_{22}e^{-d_1y} \sin d_2y \\
 & + b_{23}e^{-(m+Sc)y} + b_{25}e^{-ny} + b_{27}e^{-n_2y} + b_{29}e^{-n_3y} + b_{31}e^{-n_4y} \\
 & + b_{33}e^{-(n_4+d_1)y} \cos d_2y + b_{34}e^{-(n_4+d_1)y} \sin d_2y + b_{35}e^{-(n_6+d_1)y} \cos d_2y \\
 & + b_{36}e^{-(n_6+d_1)y} \sin d_2y + b_{37}e^{-(n_2+d_1)y} \cos d_2y + b_{38}e^{-(n_2+d_1)y} \sin d_2y \\
 & + b_{39}e^{-n_5y} + b_{41}
 \end{aligned}$$

$$\begin{aligned}
 u_2 = & -a_{19}e^{-c_1y} \sin y c_2 + b_{16}e^{-cy} + b_{18}e^{-my} + b_{20}e^{-Scy} - b_{21}e^{-d_1y} \sin d_2y + b_{22}e^{-d_1y} \cos d_2y \\
 & + b_{24}e^{-(m+Sc)y} + b_{26}e^{-ny} + b_{28}e^{-n_2y} + b_{30}e^{-n_3y} + b_{32}e^{-n_4y} \\
 & - b_{33}e^{-(n_4+d_1)y} \sin d_2y + b_{34}e^{-(n_4+d_1)y} \cos d_2y - b_{35}e^{-(n_6+d_1)y} \sin d_2y \\
 & + b_{36}e^{-(n_6+d_1)y} \cos d_2y - b_{37}e^{-(n_2+d_1)y} \sin d_2y + b_{38}e^{-(n_2+d_1)y} \cos d_2y \\
 & + b_{40}e^{-n_5y} + b_{42}
 \end{aligned}$$

$$|u_{12}| = (u_1^2 + u_2^2)^{\frac{1}{2}}, \quad \tan \alpha_3 = \frac{u_2}{u_1}$$

And from (20) we obtain the expression for concentration field as

$$\Re(\theta(y, t)) = e^{-Scy} (1 - \lambda a_0 (1 - e^{-my})) + \epsilon (\theta_1 \cos \omega t - \theta_2 \sin \omega t) \tag{24}$$

or

$$\Re(\theta(y, t)) = e^{-Scy} (1 - \lambda a_0 (1 - e^{-my})) + \epsilon \theta_1 \cos (\omega t + \alpha_2) \tag{25}$$

where

$$\begin{aligned}
 \theta_1 = & (a_3 + \lambda a_5) e^{-e_1y} \cos e_2y + (a_1 + a_4) e^{-e_1y} \sin e_2y \\
 & + a_3 e^{-(m+Sc)y} + \lambda (b_1 e^{-n_2y} + b_3 e^{-n_3y} + b_5 e^{-n_4y} \\
 & + (b_7 e^{-n_4y} + b_9 e^{-n_6y} + b_{11} e^{-n_2y}) e^{-d_1y} \cos d_2y \\
 & + (b_8 e^{-n_4y} + b_{10} e^{-n_6y} + b_{12} e^{-n_2y}) e^{-d_1y} \sin d_2y \\
 & + b_{13} e^{-n_5y}
 \end{aligned}$$

$$\begin{aligned}
 \theta_2 = & a_1 e^{-Scy} + (a_1 + a_4) e^{-e_1y} \cos e_2y \\
 & - (a_3 + \lambda a_5) e^{-e_1y} \sin e_2y + a_4 e^{-(m+Sc)y} \\
 & + \lambda (b_2 e^{-n_2y} + b_4 e^{-n_3y} + b_6 e^{-n_4y} \\
 & + (b_8 e^{-n_4y} + b_{10} e^{-n_6y} + b_{12} e^{-n_2y}) e^{-d_1y} \cos d_2y \\
 & - (b_7 e^{-n_4y} + b_9 e^{-n_6y} + b_{11} e^{-n_2y}) e^{-d_1y} \sin d_2y \\
 & + b_{14} e^{-n_5y}
 \end{aligned}$$

$$|\theta_{12}| = (\theta_1^2 + \theta_2^2)^{\frac{1}{2}}, \quad \tan \alpha_2 = \frac{\theta_2}{\theta_1}$$

Also from Eq. (21), the real part of the temperature field can be written as

$$\Re(\theta(y, t)) = e^{-my} \left(1 + \frac{1}{4} \epsilon \omega \right) + \epsilon (\theta_1 \cos \omega t - \theta_2 \sin \omega t) \tag{26}$$

or

$$\Re(\theta(y, t)) = e^{-my} \left(1 + \frac{1}{4} \epsilon \omega \right) + \epsilon \theta_{12} \cos (\omega t - \alpha_1) \tag{27}$$

where

$$\theta_1 = \frac{1}{4} \omega e^{-d_1y} \sin \omega t, \quad \theta_2 = \frac{1}{4} \omega e^{-d_1y} \cos \omega t$$

$$|\theta_{12}| = (\theta_1^2 + \theta_2^2)^{\frac{1}{2}} = \frac{1}{4} \omega e^{-d_1y}, \quad \tan \alpha_1 = \frac{\theta_2}{\theta_1} = \tan d_2y$$

From (23), (26) and (27) we obtain the expression for the transient velocity, transient concentration field and transient temperature respectively, when $\omega t = \pi/2$, as

$$u(y, t) = 1 + a_{13}e^{-cy} + a_{15}e^{-my} + a_{16}e^{-Scy} + a_{17}e^{-(m+Sc)y} - \epsilon u_2 \tag{28}$$

$$\theta(y, t) = e^{-Scy} (1 - \lambda a_0 (1 - e^{-my})) - \epsilon \theta_2 \tag{29}$$

$$\theta(y, t) = e^{-my} \left(1 + \frac{1}{4} \epsilon \omega \right) - \epsilon \theta_2 \tag{30}$$

Since we know the velocity distribution, we then calculate the skin friction as

$$\tau = \frac{\tau'}{\rho U_0' v_0'} = - \frac{\partial u}{\partial y} \Big|_{y=0}$$

$$\begin{aligned}
 \tau = & a_{13}c + a_{15}m + a_{16}Sc + a_{17}(m + Sc) \\
 & + \epsilon (a_{19}(c_1 + lc_2) + (b_{15} + lb_{16})c \\
 & + (b_{17} + lb_{18})m + (b_{19} + lb_{20})Sc \\
 & + (b_{21} + lb_{22})(d_1 + ld_2) \\
 & + (b_{23} + lb_{24})(m + Sc) + (b_{25} + lb_{26})n \\
 & + (b_{27} + lb_{28})n_2 + (b_{29} + lb_{30})n_3 \\
 & + (b_{31} + lb_{32})n_4 + (b_{33} + lb_{34})(n_4 + d_1 + ld_2) \\
 & + (b_{35} + lb_{36})(n_6 + d_1 + ld_2) + (b_{37} + lb_{38}) \\
 & (n_2 + d_1 + ld_2) + (b_{39} + lb_{40})n_5 e^{l\omega t}
 \end{aligned}$$

In terms of amplitude and phase of the skin friction, $\Re(\tau)$ is given by

$$\Re(\tau) = a_{13}c + a_{15}m + a_{16}Sc + a_{17}(m + Sc) - \epsilon(\tau_1 \cos \omega t + \tau_2 \sin \omega t)$$

or

$$\begin{aligned} \Re(\tau) &= (a_{16} + a_{17})Sc + a_{13}c - m(a_{15} + a_{17}) - \epsilon|\tau_{12}| \cos(\omega t - \alpha_6) \\ \tau_1 &= (b_{22} + b_{34} + b_{36} + b_{38})d_2 - a_{19}c_1 - b_{15}c - b_{17}m - b_{19}Sc + (b_{33} + b_{21} + b_{35} + b_{37})d_1 \\ &\quad - b_{23}(m + Sc) - b_{25}n - b_{27}n_2 - b_{37}n_3 - (b_{31} + b_{34})n_4 - b_{39}n_5 \\ \tau_2 &= -b_{22}n - b_{28}n_2 - b_{30}n_3 - b_{32}n_4 - b_{40}n_5 - a_{19}c_2 - b_{21}d_2 - b_{22}d_1 - b_{24}(m + Sc) \\ &\quad - b_{33}d_2 - b_{36}(n_6 + d_1) - b_{38}(n_2 + d_1) - b_{16}c - b_{18}m - b_{20}Sc - b_{34}(n_4 + d_1) - b_{35}d_2 - b_{37}d_2 \\ |\tau_{12}| &= (\tau_1^2 + \tau_2^2)^{\frac{1}{2}}, \quad \tan \alpha_6 = \frac{\tau_2}{\tau_1} \end{aligned}$$

Also since we know the concentration distribution, we then calculate the mass transport rate at the wall as

$$Sh = \frac{v_z' \xi_{z'}}{U_0' v_0'} \left(\frac{\mu_0}{\rho} \right)^{\frac{1}{2}} = \frac{\partial \theta}{\partial y} \Big|_{y=0}$$

$$\begin{aligned} Sh &= Sc + \lambda a_0 m \\ &\quad - \epsilon(-(a_3 + l(a_1 + a_4) + \lambda a_5)(e_1 + l e_2) - (a_3 + l b_4)(m + Sc) - l a_1 Sc \\ &\quad - \lambda((b_1 + l b_2)n_2 - (b_3 + l b_4)n_3 - (b_5 + l b_6)n_4 - (b_7 + l b_8)(n_4 + d_1 + l d_2) \\ &\quad - (b_9 + l b_{10})(n_6 + d_1 + l d_2) - (b_{11} + l b_{12})(n_2 + d_1 + l d_2) \\ &\quad - (b_{13} + l b_{14})n_5))e^{l \omega t} \end{aligned}$$

And in terms of amplitude and phase of mass transport at the wall, we have

$$\Re(Sh) = Sc + \lambda a_0 m - \epsilon(sh_1 \cos \omega t + 2 \sin \omega t)$$

or

$$\Re(Sh) = Sc + \lambda a_0 m - \epsilon sh_{12} \cos(\omega t - \alpha_5)$$

where

$$\begin{aligned} sh_1 &= -a_3 e_1 - a_3(m + Sc) \\ &\quad - \lambda(b_1 n_2 - b_3 n_3 - b_5 n_4 - b_7(n_4 + d_1) - b_9(n_6 + d_1) - b_{11}(n_2 + d_1) \\ &\quad - b_{13} n_5 + (b_8 + b_{10} + b_{12})d_2 + (a_1 + a_4)e_2 - a_5 e_1) \\ sh_2 &= -a_3 e_2 - a_1(Sc + e_1) - a_4 e_1 - a_4(m + Sc) \\ &\quad - \lambda(b_2 n_2 - b_4 n_3 - b_6 n_4 - b_8(n_4 + d_1) - b_{10}(n_6 + d_1) - b_{12}(n_2 + d_1) \\ &\quad - b_{14} n_5 + (b_7 + b_{11} + b_9)d_2 + (a_1 + a_4)e_2 - a_5 e_2) \\ |Sh_{12}| &= (Sh_1^2 + Sh_2^2)^{\frac{1}{2}}, \quad \tan \alpha_5 = \frac{Sh_2}{Sh_1} \end{aligned}$$

Finally, expression for heat transfer at the wall is written as

$$\begin{aligned} Nu &= -\frac{\partial \theta}{\partial y} \Big|_{y=0} \\ Nu &= m + \frac{1}{4} l \epsilon \omega (d_1 + l d_2 + m) e^{l \omega t} \end{aligned}$$

In terms of amplitude and phase of the skin friction, we have

$$\Re(Nu) = m - \epsilon(Nu_1 \cos \omega t - Nu_2 \sin \omega t)$$

or

$$\Re(Nu) = m - \epsilon Nu_{12} \cos(\omega t - \alpha_4)$$

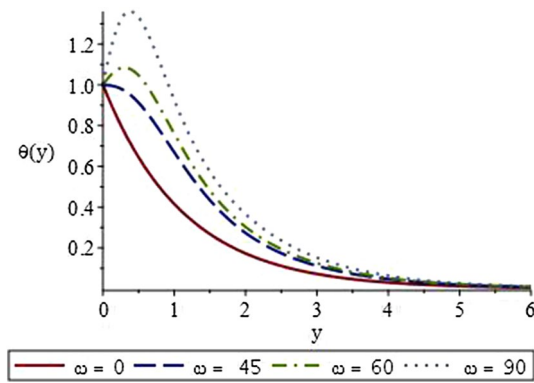


Fig. 1 Temperature distribution at different ω

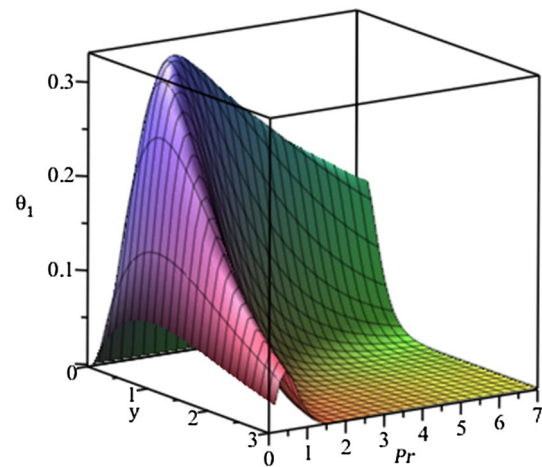


Fig. 3 Temperature phase distribution

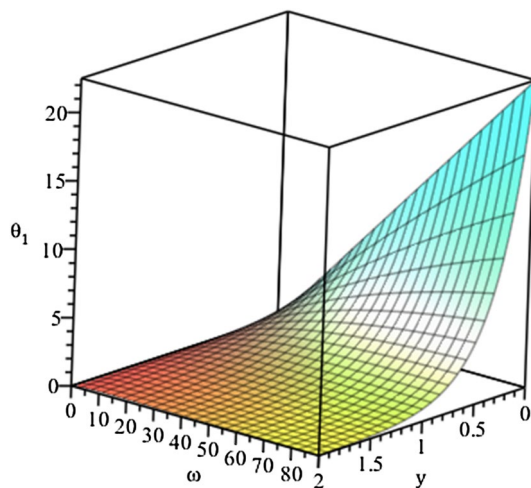


Fig. 2 Temperature amplitude at different ω

where

$$Nu_1 = \frac{1}{4} \epsilon \omega d_2$$

$$Nu_2 = \frac{1}{4} \epsilon \omega (m - d_1)$$

$$|Nu_{12}| = (Nu_1^2 + Nu_2^2)^{\frac{1}{2}} = \frac{1}{4} \epsilon \omega (d_2^2 + (m - d_1)^2)^{\frac{1}{2}},$$

$$\tan \alpha_4 = \frac{Nu_2}{Nu_1} = \frac{d_2}{m - d_1}$$

4 Discussion of results

The influence of an increment in the various parameters values $V, M, k_p, A, \delta, Gr_t, Gr_c, \lambda, r$ and ω on the behavior of the flow fluid for fixed values of Sc, Pr and ϵ are carried out. To obtain the impact of the terms on the flow characteristic, for practical purpose, the Schmidt number is chosen as $Sc = 0.62$ while the Prandtl number is taken as $Pr = 0.71$ at

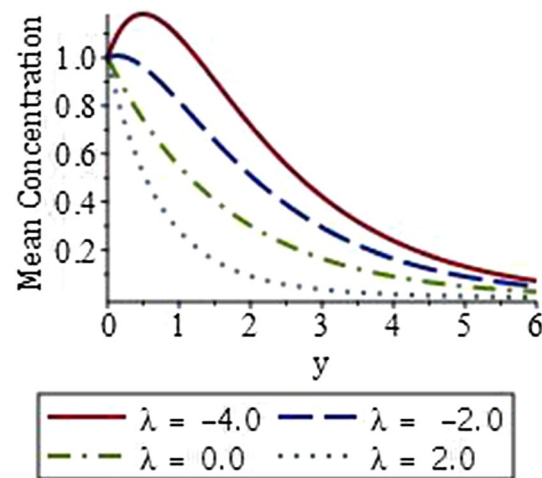


Fig. 4 Mean concentration distribution for various λ

a single atmospheric pressure depicting the air at temperature 25 °C. For simplicity, $|\psi_{12}| \equiv \psi_{12}$, where $\psi = u, \theta$ and θ . The default values of the parameters are taken as follows: $V = 0.3, M = 0.2, k_p = 0.5, A = 0.5, \delta = 0.2, Gr_t = 0.5, Gr_c = 0.2, \lambda = 0.1, r = 1.0$ and $\omega = \pi t$ with unvaried value of $\epsilon = 0.05$ and $Pr = 0.71$ and unless otherwise stated.

4.1 Temperature field

In Fig. 1, we display the transient temperature field with various values of angular velocity ω . It is seen that temperature increases as the liquid angular velocity increases and the temperature boundary layer decreases as the fluid moves away from the plate which is asymptotically as it approaches zero far away. The occurrence of peak heat profile shows that maximum fluid temperature exists as found in the plot. Also, temperature boundary

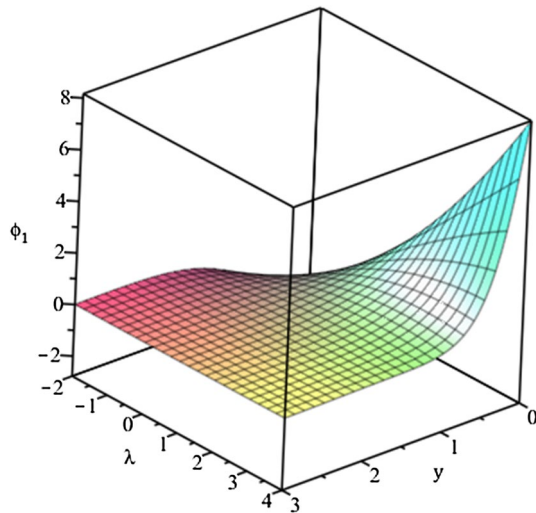


Fig. 5 Concentration phase distribution

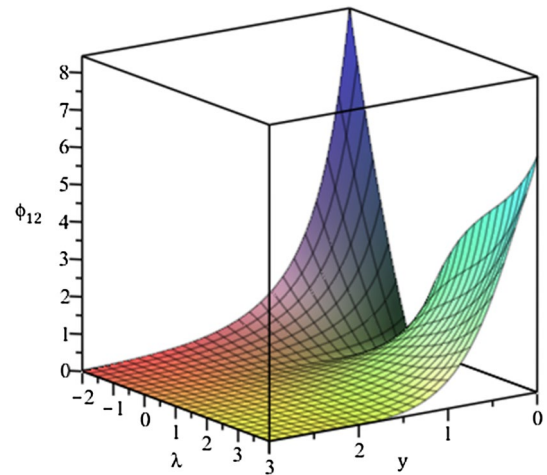


Fig. 7 Mean concentration phase distribution

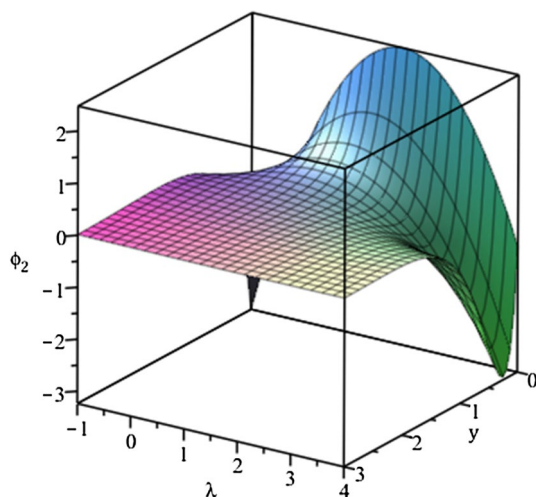


Fig. 6 Mean concentration phase distribution

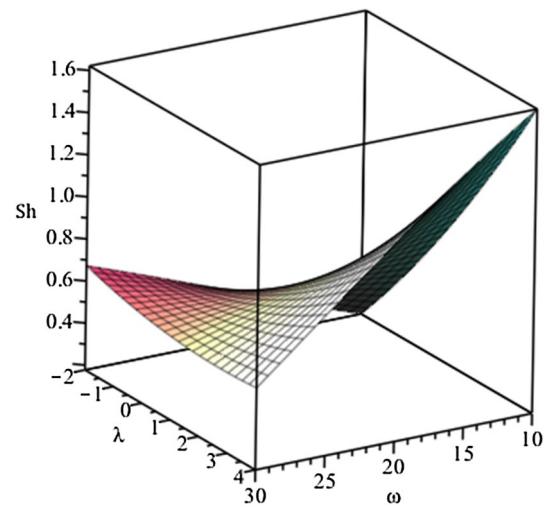


Fig. 8 Rate of mass transfer at the wall

layer increases with a rise in the term ω . Figure 2 shows the influence of the parameter ω on heat amplitude. We could see that maximum amplitudes occur when $\omega > 45$. This maximum is given by $(\omega^2 + 16)/(16(4\epsilon + 1))$. The fluctuating part of the temperature is shown in Fig. 3. It is noticed from this figure that the heat boundary layer reduces as the Prandtl number rises. Temperature fluctuating part also diminishes with rises in the Prandtl number. It should also be mentioned that temperature increases for an increase in heat generation (i.e. $\delta > 0$) and vice versa as well, the phase angle also increases with increase in Prandtl number.

4.2 Concentration field

Mean concentration distribution variation with reverence to chemical reactivity is displayed in Fig. 4. It could be seen that fluid concentration is encouraged with enhancement in the chemical generative reaction and discourage with rises in the chemical destructive reaction. We also observed that for higher value of negative λ , corresponding to generative chemical reaction, maximum fluid concentration exist near the plate. Figures 5, 6 and 7 display the concentration phase and phase amplitude with respect to chemical reactivity. It could be seen that

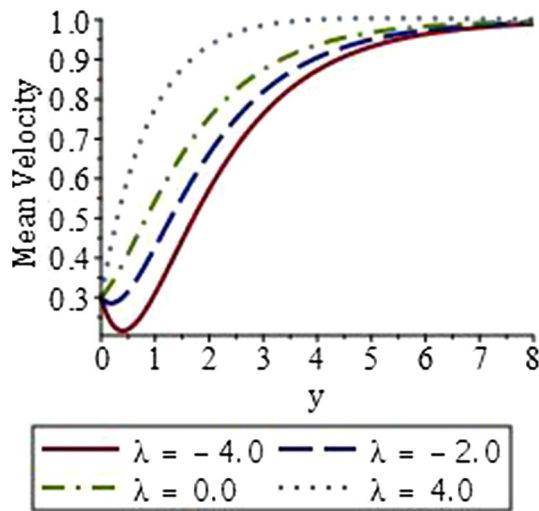


Fig. 9 Mean velocity distribution for various values of λ

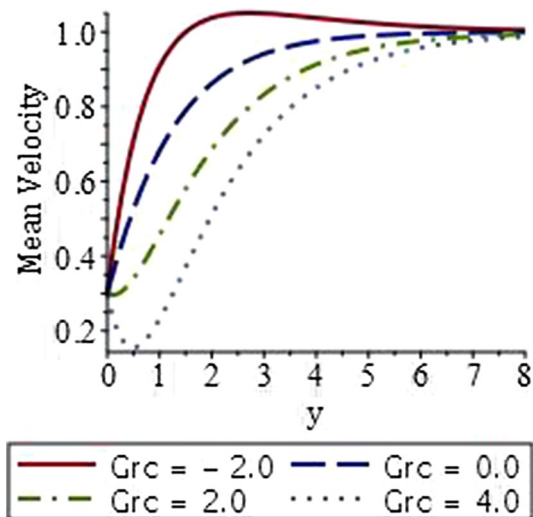


Fig. 11 Mean velocity distribution for various values of Grc

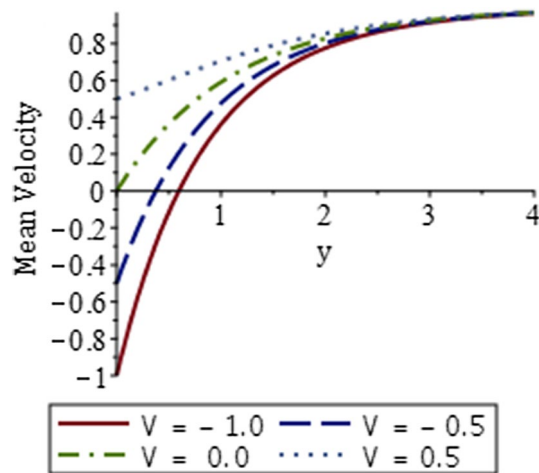


Fig. 10 Mean velocity distribution for various values of V

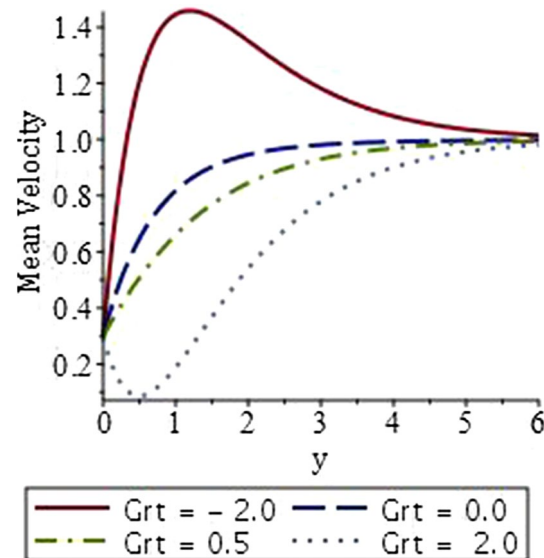


Fig. 12 Mean velocity distribution for various values of Grt

concentration phase diminishes with rise in the generative chemical reaction, it increases with rise in the destructive chemical reaction as shown in Fig. 5 but oscillatory phase 2 decreases with increase in reactivity parameter either destructive or generative reaction as presented in Fig. 6. The amplitude of the concentration phase is seen to increase with increase in reactivity parameter as shown in Fig. 7. The rate of species transport at the wall, as shown in Fig. 8 indicate that mass transfer at the wall decrease with generative chemical reaction and increases with destructive chemical reaction.

4.3 Velocity field

The mean velocity distributions are demonstrated in Figs. 9, 10, 11 and 12 for various values of the parameters,

reactivity λ , magnetic M , surface limiting velocity V , thermal and mass Grashof numbers (Grt, Grc) and permeability k_p . It worth nothing that variations in the transient momentum with flow parameters are the same with mean velocity, thus we choose mean velocity variation for our discussion. In Fig. 9, it could be noticed that mean velocity decrease with a rise in the generative chemical reaction and increases with a rise in the chemical reaction destructive. From Fig. 10, it is realized that the mean momentum rises as the sheet motions in the flow direction; however it reduces as it motions in the direction opposite the flow. The effect of Grashof number was shown in Figs. 11 and

12, in the figures, we see that the flow rate diminishes with a boost in the mass buoyancy and thermal buoyance number for a heated surface ($Grt > 0$), while the plate cools at ($Grt < 0$) resulted in decrease in the flow rate as the plate cooling rate rises.

4.4 Skin friction

The Skin Friction τ is plotted for against free stream oscillation ω for the time parameter A and solutant buoyance number Grc as presented in Figs. 13 and 14. It is noticed that the skin friction τ decrease with an increase in the parameter values A . Increase in mass buoyancy is seen to decrease the skin friction due to thinner in the momentum boundary layer. The fluctuating part of skin friction τ_2 is displayed in Figs. 15 and 16. It is observed from Fig. 15 that an increase in the solutant buoyance number resulted in

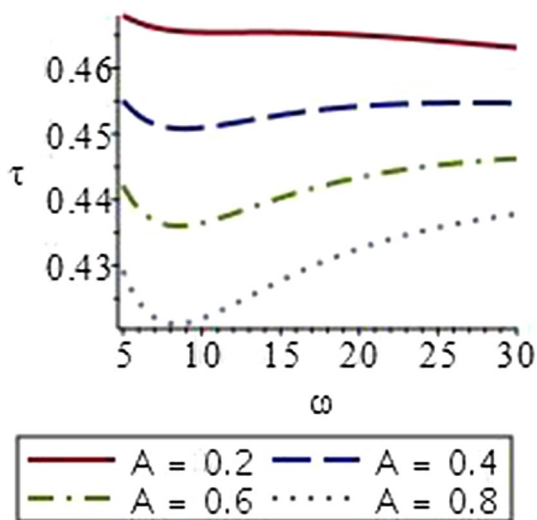


Fig. 13 Skin-friction for various values of A

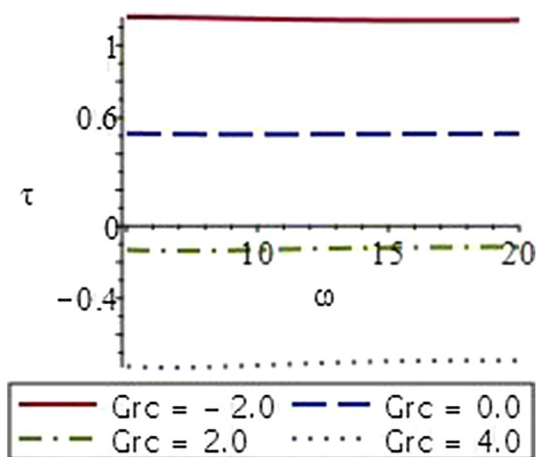


Fig. 14 Skin-friction for various values of Grc

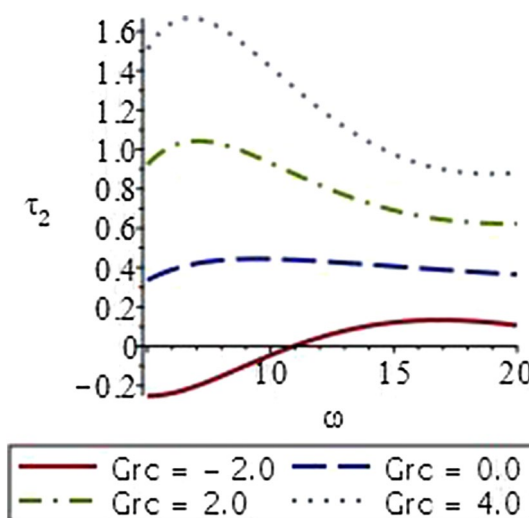


Fig. 15 Skin-friction phase for various values of Grc

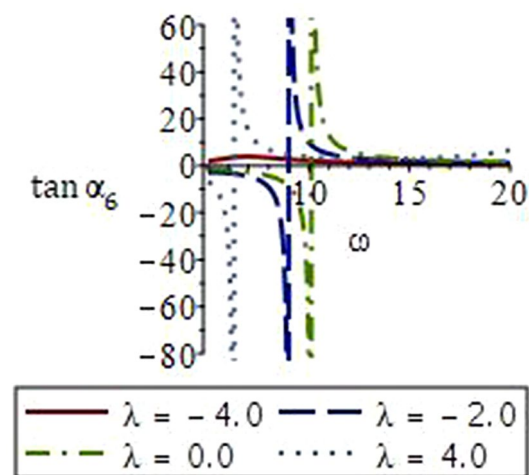


Fig. 16 Skin-friction phase angle for various values of λ

an increase in the skin friction fluctuation part τ_2 . Skin friction phase angle varied with respect to reactivity parameter and reaction order are shown in Fig. 16. It is seen that the phase angle increases with reactivity parameter and decrease with reaction order.

5 Conclusions

In this study, we have studied analytically the energy and species transfer in unsteady boundary layer flow of natural convection MHD fluid past a motioning sheet with chemical binary reaction. The liquid surface is impulsively motioned with an unvaried velocity in either the flow opposite direction or fluid flow direction in the occurrence

of perpendicular magnetic field. With oscillating fluid flow, we can study both frequency-dependent effects and “long-time” effects that would require non-practically long channels to be observed in steady flow. We explore mathematically important aspects of reaction engineering in reactive flow, especially residence time flow behaviour, scale-up and scale-down procedures. The following deduction are made from the study:

- Temperature increases as the fluid angular velocity increases.
- Maximum temperatures exist in the body of the fluid.
- Concentration increases with a rise in the generative chemical reaction and vice versa.
- Concentration phase reduces with an enhancement in the in generative chemical reaction.
- Amplitude of concentration phase increase with increase in reactivity parameter.
- Mean velocity decrease with a rise in chemical reaction generative and reaction order.
- Velocity diminishes with increase in mass buoyance and thermal Grashof number for heating of the plate.
- Skin-friction increases as generative/destructive chemical reaction increases.
- Skin friction increases as limiting surface moves in opposite direction and decreases as the limiting surface motions in the fluid flow direction.

Compliance with ethical standards

Conflict of interest All authors have agreed and approved the manuscript, and have contributed significantly towards the article. There is no conflict of interest among the authors.

References

1. Salawu SO, Ogunseye HA, Olanrewaju AM (2018) Dynamical analysis of unsteady poiseuille flow of two-step exothermic non-newtonian chemical reactive fluid with variable viscosity. *Int J Mech Eng Technol* 9:596–605
2. Hassan AR, Gbadeyan JA, Salawu SO (2018) The effects of thermal radiation on a reactive hydromagnetic internal heat generating fluid flow through parallel porous plates. *Springer Proc Math Stat* 259:183–193
3. Salawu SO, Fatunmbi EO (2017) Inherent irreversibility of hydro-magnetic third-grade reactive poiseuille flow of a variable viscosity in porous media with convective cooling. *J Serbian Soc Comput Mech* 11:46–58
4. Soundalgekar VM, Martin BW, Gupta SK, Pop I (1976) On unsteady boundary layer in a rotating fluid with time dependent suction. *Publ De L'Inst Math* 20:215–226
5. Bergstrom RW (1976) Viscous boundary layers in rotating fluids driven by periodic flows. *J Atmos Sci* 33:1234–1247
6. Nazar R, Amin N, Pop I (2004) Unsteady boundary layer flow due to a stretching surface in a rotating fluid. *Mech Res Commun* 31:121–128
7. Abbas Z, Javed T, Sajid M, Ali N (2010) Unsteady MHD flow and heat transfer on a stretching sheet in a rotating fluid. *J Taiwan Inst Chem Eng* 41:644–650
8. Zheng L, Li C, Zhang X, Gao Y (2011) Exact solutions for the unsteady rotating flows of a generalized Maxwell fluid with oscillating pressure gradient between coaxial cylinders. *Comput Math Appl* 62:1105–1115
9. Makinde OD, Olanrewaju PO (2011) Unsteady mixed convection with Soret and Dufour effects past a porous plate moving through a binary mixture of chemically reacting fluid. *Chem Eng Commun* 198:920–938
10. Makinde OD, Olanrewaju PO, Charles WM (2011) Unsteady convection with chemical reaction and radiative heat transfer past a flat porous plate moving through a binary mixture. *Africka Matematika* 22:65–78
11. Chamkha AJ, Rashad AM, Al-Mudhaf H (2012) Heat and mass transfer from truncated cone with variable wall temperature and concentration in the presence of chemical reaction effects. *Int J Numer Methods Heat Fluid Flow* 22:357–376
12. Waqas H, Khan SU, Imran M, Bhatti MM (2019) Thermally developed Falkner–Skan bioconvection flow of a magnetized nanofluid in the presence of motile gyrotactic microorganism: Buongiorno's nanofluid model. *Phys Scr* 94(11):432–443
13. Nguyen TK, Bhatti MM, Ali JA, Hamad SM, Sheikholeslami M, Shafee A (2019) Macroscopic modeling for convection of Hybrid nanofluid with magnetic effects. *Phys A* 534:122136. <https://doi.org/10.1016/j.physa.2019.122136>
14. Nguyen-Thoi T, Bhatti MM, Ali JA, Hamad SM, Sheikholeslami M, Shafee A, Haq R-U (2019) Analysis on the heat storage unit through a Y-shaped fin for solidification of NEPCM. *J Mol Liq* 292:111378
15. Maleque KA (2013) Unsteady natural convection boundary layer flow with mass transfer and a binary chemical reaction. *Br J Appl Sci Technol* 3:131–149
16. Maleque KA (2014) A binary chemical reaction on unsteady free convective boundary layer heat and mass transfer flow with arrhenius activation energy and heat generation or absorption. *Lat Am Appl Res* 44:97–104
17. Awad FG, Motsa S, Khumalo M (2014) Heat and mass transfer in unsteady rotating fluid flow with binary chemical reaction and activation energy. *PLoS ONE* 9:234–244
18. Mallikarjuna B, Rashad AM, Chamkha AJ, Raju SH (2015) Chemical reaction effects on MHD convective heat and mass transfer flow past a rotating vertical cone embedded in a variable porosity regime. *Afrika Matematika* 27:645–653
19. Zhang C, Zheng L, Zhang X, Chen G (2015) MHD flow and radiation heat transfer of nanofluid in porous media with variable surface heat flux and chemical reaction. *Appl Math Model* 39:165–172
20. Abbas Z, Sheikh M, Motsa SS (2016) Numerical solution of binary chemical reaction on stagnation point flow of Casson fluid over a stretching/shrinking sheet with thermal radiation. *Energy* 95:12–20
21. Shafique Z, Mustafa M, Mushtaq A (2016) Boundary layer flow of Maxwell fluid in rotating frame with binary chemical reaction and activation energy. *Results Phys* 6:627–633
22. Khan N, Mahmood T, Sajid M, Hashmi MS (2016) Heat and mass transfer on MHD mixed convection axisymmetric chemically reactive flow of Maxwell fluid driven by exothermal and isothermal stretching disks. *Int J Heat Mass Transf* 92:1090–1105

23. Mabood F, Shateyi S, Rashidi MM, Momoniat E, Freidoonimehr N (2016) MHD stagnation point flow heat and mass transfer of nanofluids in porous medium with radiation, viscous dissipation and chemical reaction. *Adv Powder Technol* 27:742–751
24. Rawat S, Kapoor S, Bhargava R (2016) MHD flow heat and mass transfer of micropolar fluid over a nonlinear stretching sheet with variable micro inertia density, heat flux and chemical reaction in a non-darcy porous medium. *J Appl Fluid Mech* 9:321–331
25. Messiha SAS (1994) Laminar boundary layers in oscillatory flow along an infinite flat plate with variable suction. *Proc Camb Philos Soc* 62:329–337
26. Lighthill MJ (1954) The response of laminar skin friction and heat transfer to fluctuations in the stream velocity. *Proc R Soc Lond A* 224:1–23

Publisher's Note Springer Nature remains neutral with regard to jurisdictional claims in published maps and institutional affiliations.